

A Voltage-Induced Transition of Hemin in BIODÉ (Biomolecular Light-Emitting Diode)

Hiroyuki Tajima,* Kazuhiro Shimatani, Takeshi Komino, Masaki Matsuda, Shingo Ikeda, Yoriko Ando, and Hidefumi Akiyama

The Institute for Solid State Physics, The University of Tokyo, 5-1-5 Kashiwanoha, Kashiwa 277-8581

Received July 25, 2005; E-mail: tajima@issp.u-tokyo.ac.jp

We fabricated biomolecular light-emitting diodes (BIODE) using hemin, and measured the electroluminescence (EL) spectra, current–voltage and EL intensity–voltage characteristics. The current–voltage and EL intensity–voltage characteristics revealed an irreversible transition of hemin for the applied voltage of $V \approx 4.5$ V, above which drastic changes of the EL spectra occur. In order to clarify the origin of this voltage-induced transition, we determined the spin state of several compounds containing heme (hemin, myoglobin, and cytochrome *c*) using magnetic susceptibility and Raman spectra. We clarified the features of the EL spectra of heme compounds both in the oxidized low-spin state and in the oxidized high-spin state. Based on the spectral features thus obtained, we concluded that the voltage-induced transition in hemin is associated with the change of iron from the oxidized high-spin state ($S = 5/2$) to the oxidized low-spin state ($S = 1/2$).

The thin-film organic light-emitting diode (OLED) was fabricated by Vincett et al. for the first time.¹ In this device, light emission occurs through the recombination process of electron–hole pairs injected from electrodes (electroluminescence = EL). Based on this principle, most of the EL studies intend to produce devices with various colors and with high efficiencies. The fabricated devices are equipped with electron- and hole-transport layers, and sometimes with multi-emission layers. The EL spectra as well as quantum efficiencies are no more the intrinsic properties of materials in these devices. On the other hand, the OLED technique is a new spectroscopy of potential use for insulating materials. For this purpose, the transport layers are not always necessary and an OLED with a simple metal/insulator/metal junction has some advantage. However, such EL studies are quite few at present.

We recently succeeded in obtaining the EL spectra of cytochrome *c* (Fig. 1c).² This is the first report on the fabrication of a biomolecular light-emitting diode (BIODE). Subsequently, we fabricated BIODÉ devices using other porphyrin-containing biomolecules (myoglobin³ (Fig. 1b), chlorophyll *a*⁴) and reported the EL spectra of the compounds. Interestingly, heme proteins (heme = iron porphyrin) do not or hardly exhibit photoluminescence (PL), although chlorophyll *a*, which does not contain iron, exhibits PL. In the last paper,⁵ we proposed a model in which the excitation process of EL in heme is different from that of PL. We concluded that the difference explains why heme compounds exhibit EL but not PL.

In this paper, we report on the EL external quantum efficiency and the EL spectra of BIODÉ devices fabricated from hemin ($\text{C}_{34}\text{H}_{32}\text{Cl Fe}^{\text{III}} \text{N}_4\text{O}_4$; MW = 651.94). Hemin is a small molecule containing an iron protoporphyrin IX unit (See the molecular structure shown in Fig. 1a). There are no PL studies reported on this molecule. We show that the EL spectrum of hemin changes under applied voltages. This spectral change is attributable to a transition from the high-spin state to the low-spin state.

Experimental

Hemin and Myoglobin were purchased from Sigma Co. (chlorohemin >80%; myoglobin from skeletal muscle, 95–100%). Cytochrome *c* was purchased from Wako Pure Chemical Industries, Ltd. (horse-heart cytochrome *c*, crystalline powder). Our preliminary experiments revealed that PL in these compounds is too small to be detected.

A thin film of hemin was fabricated on an ITO electrode from a methanol solution by a spin-coating technique. The ITO (indium tin oxide)/hemin/Al junction was completed by the vacuum deposition of an Al film on the hemin film. Details on the device fabrication for cytochrome *c* and myoglobin have been reported elsewhere.^{2,3,5} The current–voltage characteristics were measured using a volt meter (34420A, Agilent Technology) and a programmable electric source (7651, Yokogawa). The emission intensity was estimated using a Si photo-diode sensor and an electrometer (TR8652, Advantest). The EL spectra were measured using a 15 cm monochromator and a nitrogen-cooled back-illumination-type CCD (Roper scientific). The Raman spectra were measured using a Ramascope System 1000 (Renishaw). An Ar⁺ laser (514.5 nm) was used for the excitation. The magnetic susceptibility measurements were performed using MPMS (Quantum Design). The surface observation and the thickness measurements for the fabricated hemin films were carried out using an atomic force microscope (AFM), Nanopics 2100 (SII Nanotechnology Inc.).

Results

AFM Image of a Hemin Film. Figure 2 shows (a) an AFM image of a hemin film fabricated on an ITO electrode, and (b) a schematic illustration of a hemin BIODÉ fabricated in this study. The average thickness of the film was 30–45 nm. This thickness was approximately the same as that of the cytochrome *c* or myoglobin films in the BIODÉ devices studied previously.^{2,3} The grain sizes of a hemin film were much larger than those of cytochrome *c* and myoglobin films.^{2,3}

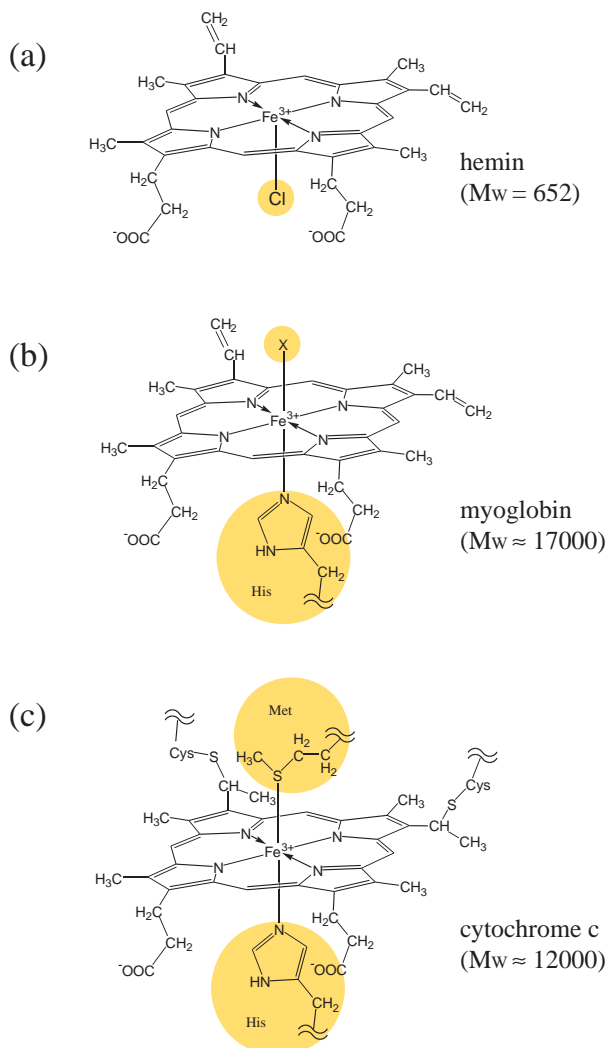


Fig. 1. The molecular structures of (a) hemin, (b) ferrimyoglobin, and (c) ferricytochrome *c*.

However, most of the fabricated devices worked without any short circuits.

Current–Voltage Characteristics, EL Intensity–Voltage Characteristics, and External Quantum Efficiency of a Hemin BIODE. Figures 3a, 3b, 3d, and 3e show the current–voltage and the EL intensity–voltage characteristics of the ITO/hemin/Al junction for two samples (#1 and #2). In sample #1, the current was drastically increased above $V = 9$ V, and the junction was seriously damaged. As for sample #2, we cyclically changed the bias voltages between 0 and 7 V [$0\text{ V} \rightarrow 5.4\text{ V} \rightarrow 0\text{ V} \rightarrow 6.9\text{ V} \rightarrow 0\text{ V} \rightarrow 7\text{ V} \rightarrow 0\text{ V}$]. In both samples, the current and light intensity at the initial sweep gradually increased above $V \approx 3$ V, took a peak around $V = 4.5$ V, and gradually increased again above $V \approx 5.5$ V. Similar behavior was observed in other samples studied.

Figures 3c and 3f show the voltage dependence of the external quantum efficiency of the hemin BIODE. The external quantum efficiency of OLED is defined as the probability that a single photon is emitted when a single electron passes across the junction. This quantity is proportional to the EL intensity and inversely proportional to the current. In the initial sweep

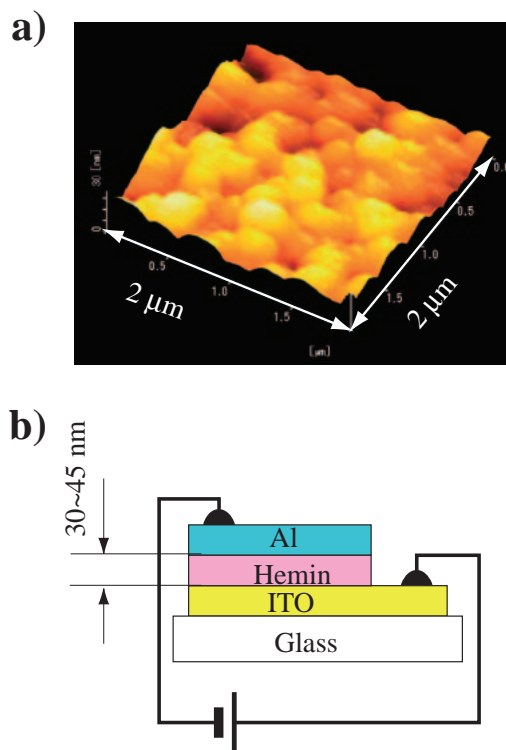


Fig. 2. (a) An AFM image of a hemin film formed on the ITO electrode; (b) a schematic illustration of ITO/hemin/Al junction fabricated in this study.

of the voltages, the quantum efficiency took a peak around $V = 5$ V, and then drastically decreased, and again gradually increased above $V \approx 6$ V. Hereinafter, we call the state observed below 5 V as the low-voltage (LV) state and the state observed above 5 V as the high-voltage (HV) state, respectively. As can be seen from Fig. 3f, the voltage-induced transition of hemin was irreversible, and the LV state is observed only in the initial sweep of the voltage. In the HV state, the quantum efficiencies as a function of voltages are consistent for all the voltage cycles, although current–voltage and EL intensity–voltage characteristics are not reproducible. We have already reported similar behavior for cytochrome *c*⁵ and myoglobin.³

As shown later, EL spectra of hemin in the HV state are associated with the heme in the low-spin state. Thus, it may be informative to compare the quantum efficiency of a hemin BIODE in the HV state with that of a BIODE containing a low-spin heme protein (cytochrome *c* or myoglobin). The quantum efficiencies of cytochrome *c* and myoglobin BIODE devices are almost the same, and are $\approx 3 \times 10^{-8}$ at $V = 10$ V.^{3,5} Thus, the efficiency of the hemin BIODE in the HV state is comparable to that of a heme-protein BIODE. Since the light emission is attributable to the heme unit in these BIODE devices, the electrical conduction not through the heme unit should reduce the external quantum efficiency. Considering a big difference in molecular sizes between hemin and heme proteins, a similar value of the quantum efficiency strongly suggests that the dominating electrical conduction in these BIODE devices is a hopping type, and most of the electric carriers pass through the heme unit.

EL Spectra of Hemin, Myoglobin, and Cytochrome *c*. In

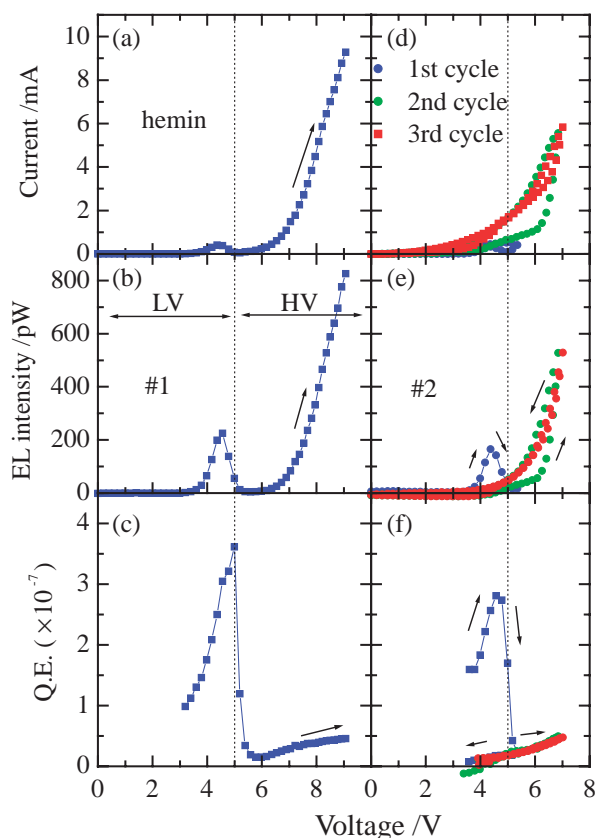


Fig. 3. Current–voltage (a and d), EL intensity–voltage (b and e), and quantum efficiency–voltage characteristics (c and f) of the ITO/hemin/Al junction for two samples (#1 and #2). The voltage cycle was repeated three times for the sample #2.

order to examine the origin of the voltage-induced transition, we measured the EL spectra in both LV and HV states. Figures 4a and 4b show the EL spectra obtained for two hemin BODE devices. Figures 4c and 4d show the EL spectra of myoglobin³ and cytochrome *c*^{2,5} BODE devices for comparison. The EL spectra of hemin in the LV state are composed of several narrow bands. Although the spectrum in the LV state shown in Fig. 4a has a tail below 550 nm, this is probably due to the mixing of the HV-state spectrum into the LV-state spectrum during the spectrum accumulation in CCD. The EL spectra of hemin in the HV state exhibit broad peaks. The spectral features in the HV state are very similar to those of cytochrome *c* and myoglobin.

Magnetic Susceptibility and Raman Spectra of Hemin, Myoglobin, and Cytochrome *c* (Determination of the Spin State). The spectral changes associated with the applied voltages remind us of the transition from a low-spin state into a high-spin state in the compounds containing iron porphyrins. The native form of cytochrome *c* is a low-spin compound of iron.⁶ Both the high-spin and low-spin states are known in myoglobin.⁷ Hemin is a high-spin five-coordinate compound of iron.⁸ However, the spin state of these compounds is very subtle and easily changes when the substitution or addition of ligands occurs.⁷ Thus, in order to ascertain the spin state of the compounds used for the device fabrication, we measured the magnetic susceptibility and Raman spectra of the compounds.

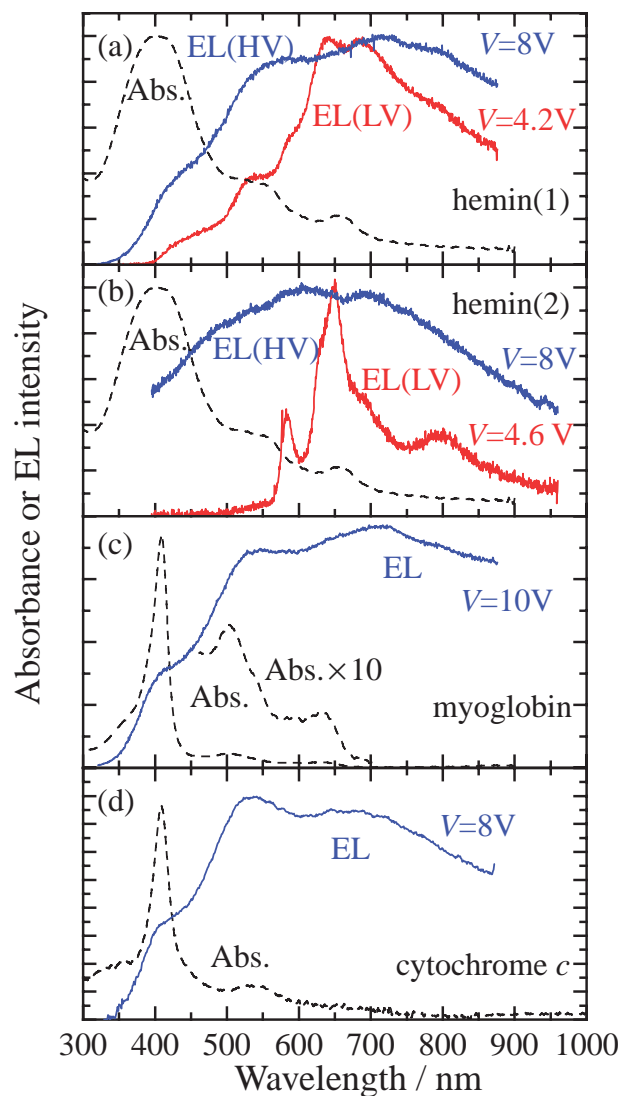


Fig. 4. The EL and the absorption spectra of hemin (sample 1, 2; a, b); myoglobin (c); cytochrome *c* (d). The absorption spectra were measured for samples in films (a, b, and d) or in solution (c).

Magnetic susceptibility gives us direct information about whether a sample is in the low-spin state or in the high-spin state. Figure 5 shows the magnetic susceptibility of the powder sample of hemin, myoglobin, and cytochrome *c* used for the device fabrication. We analyzed the susceptibility data by fitting to the Curie–Weiss law $\chi(T) = \chi_0 + C/(T - \Theta)$. The obtained parameters are listed in Table 1. From the Curie constant, C , we evaluated the effective magnetic moment by using $\mu_{\text{eff}} = \sqrt{3k_B C/N}$. This value is also listed in Table 1. The estimates of the effective magnetic moment, using $\mu_{\text{eff}} = g_{\text{eff}} \sqrt{S(S+1)} \mu_B$ are $\mu_{\text{eff}} = 2.00 \mu_B$ (low-spin Fe^{3+} ; $g_{\text{eff}} = 2.31$; $S = 1/2$) and $\mu_{\text{eff}} = 5.92 \mu_B$ (high-spin Fe^{3+} ; $g_{\text{eff}} = 2$; $S = 5/2$). Here, the g_{eff} value in the low-spin state is estimated from the g -tensor obtained in the ESR studies⁹ by $g_{\text{eff}} = \{(g_{xx}^2 + g_{yy}^2 + g_{zz}^2)/3\}^{1/2}$. In the case of the high-spin state, a detailed analysis shows that the effective magnetic moment decreases below $\approx 20 \text{ K}$.¹⁰ However, this effect was not so serious at least in the estimation of the Curie constant.¹¹ From

the analyses shown above, we concluded that the iron in hemin was in the high-spin state ($S = 5/2$). In the case of cytochrome *c* and myoglobin, the obtained effective magnetic moments did not coincide either to the high-spin value or to the low-spin value. Since the high-spin state was not plausible in cytochrome *c*, we considered that a small deviation of the effective magnetic moment in cytochrome *c* was due to the partial orientation of polycrystalline samples in the magnetic field. If such orientation occurs, the observed effective magnetic moment should increase, because the *g*-tensor of cytochrome *c* is highly anisotropic. In the case of myoglobin, the four (reduced low-spin [$S = 0$]; reduced high-spin [$S = 2$]; oxidized low-spin [$S = 1/2$]; oxidized high-spin [$S = 5/2$]) states are known.⁷ One may consider that the iron in the reduced state was the cause. As we discuss later, however, this possibility was excluded from the assignments of the 1374 cm^{-1} band in the Raman spectra. Then, we assumed that iron in the myoglobin was a mixture of high-spin Fe^{III} and low-spin Fe^{III} . Based on this assumption, we estimated that 91% of the Fe atoms in myoglobin were low-spin Fe^{III} ($S = 1/2$), and that

9% of the Fe atoms were high-spin Fe^{III} ($S = 5/2$).¹²

Raman spectra analysis is another method to determine the oxidation and spin states of iron in heme. In this method, the iron state in heme is determined from some marker bands in the spectra. This is an indirect method, but advantageous for the application to films. We measured the Raman spectra of samples in powder, and in films fabricated on aluminum. Here, we should note that a hemin film is formed not on an aluminum electrode, but on an ITO electrode when we fabricate a BIODE device. One may consider that a film formed on ITO is different from that formed on aluminum in properties, since the influence of a substrate on a film is generally recognized. However, we consider that the hemin films formed on ITO and aluminum substrates are essentially the same based on the following reasons. First, an aluminum substrate is covered with Al_2O_3 , which has properties similar to In_2O_3 in ITO. Second, the spin-coating technique tends to form random-orientation films. This indicates that the effect of substrates on films is not so serious in this wet-process method.

Figure 6 shows the Raman spectra of hemin, myoglobin, and cytochrome *c*. First, we focus on the Raman spectra of powder samples for hemin and myoglobin, both of which have the iron protoporphyrin IX skeleton. According to the literatures,^{13,14} the Raman band attributable to the C–N stretching mode reflects the oxidation state of the iron in the porphyrin ring. This band appears at 1360 cm^{-1} in the reduced myoglobin and at 1374 cm^{-1} in the oxidized myoglobin. The corresponding Raman band in Fig. 6 appears at 1371 cm^{-1} for both hemin and myoglobin powder. No split of the band is observed. Thus, we concluded that Fe^{III} was the iron state in these powder samples. In the range of $1500\text{--}1630\text{ cm}^{-1}$, there are two kinds of intense spin-marker bands, both attributable to the C–C stretching mode of the porphyrin ring. One of the spin-marker bands appears around 1566 cm^{-1} in the six-coordinated high-spin state, around 1574 cm^{-1} in the five-coordinated high-spin state, and around 1585 cm^{-1} in the six-coordinated low-spin state.¹⁵ The position of this spin-marker band is not affected by the oxidation state. Another spin-marker band around 1630 cm^{-1} is sensitive to both spin and oxidation states.^{13,16} When the oxidation state is the same, this band appears at lower frequency in the high-spin state than in the low-spin state. As shown in Fig. 6a, the spin-marker bands appear at 1570 and 1630 cm^{-1} in hemin. This suggests that the hemin sample was in the five-coordinated high-spin state. The spin-marker bands in myoglobin appear at 1560 , 1585 , and 1640 cm^{-1} . The intensity of the 1560 cm^{-1} band is considerably weaker than the other two bands. This spectrum suggests that most parts of the myoglobin sample were in the low-spin state, although a small portion of myoglobin was in the high-spin state. These conclusions obtained for both hemin and myo-

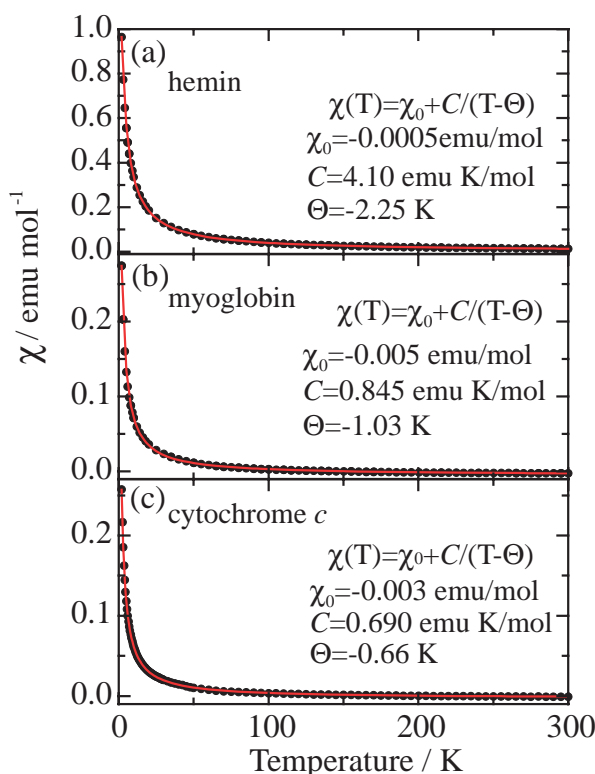


Fig. 5. The magnetic susceptibility of powder samples of (a) hemin, (b) myoglobin, and (c) cytochrome *c* used for the device fabrications.

Table 1. Curie–Weiss Parameters (χ_0 , C , and Θ) Derived from the Magnetic Susceptibility, and Effective Magnetic Moment Evaluated from C Using $\mu_{\text{eff}} = \sqrt{3k_B C/N}$

	χ_0 /emu mol ⁻¹	C /emu K mol ⁻¹	Θ /K	μ_{eff} / μ_B	Spin state HS: high spin ($S = 5/2$) LS: low spin ($S = 1/2$)
hemin	-0.0005	4.10	-2.25	5.74	HS
myoglobin	-0.005	0.845	-1.03	2.60	LS(91%) + HS(9%)
cytochrome <i>c</i>	-0.003	0.690	-0.66	2.35	LS

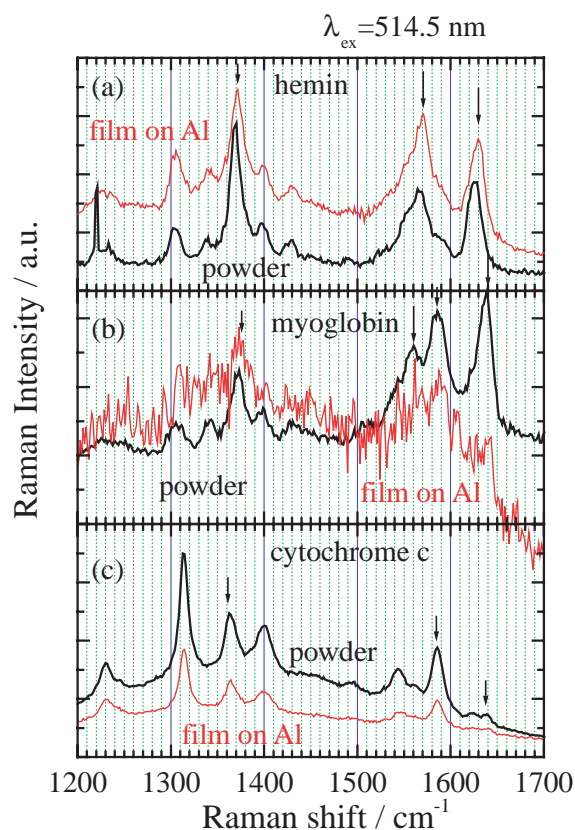


Fig. 6. The Raman spectra of (a) hemin, (b) myoglobin, and (c) cytochrome *c* for powder and film samples.

globin are qualitatively consistent with the results of magnetic susceptibility measurements.

Now, we go to the oxidation and spin state of films for hemin and myoglobin. The Raman spectrum of hemin film was almost consistent with that of the powder sample. We thus concluded that the hemin film was in the oxidized high-spin state. In the case of the myoglobin film, the S/N ratio of the spectrum is quite poor. However, it is obvious that there are vibrational bands at 1374, 1585, and 1640 cm^{-1} . Thus, we concluded that a majority of myoglobin in film was in the oxidized low-spin state. This conclusion is consistent with the experiments reported by Feng et al.¹³

Cytochrome *c* has heme *c*, a saturated porphyrin ring. The spin-marker band in the saturated porphyrin ring appears at 1575 cm^{-1} in the six-coordinated high-spin state, and at 1584 cm^{-1} in the five-coordinated low-spin state, and at 1590 cm^{-1} in the six-coordinated low-spin state.¹⁵ The difference of the Raman shift between the five-coordinated high-spin heme and the six-coordinated low-spin heme is only 6 cm^{-1} , which is beyond the accuracy of our Raman experiments. Therefore, we could not determine the spin state directly from the measured Raman spectra. Instead, we compared the Raman spectrum of the powder sample with that of the film sample, and concluded that the two samples were in the same spin state. Since the magnetic susceptibility data explicitly showed that the powder sample of cytochrome *c* was in the oxidized low-spin state, we concluded that the fabricated film of cytochrome *c* was also in the same state.

Discussion

Based on the conclusion for the spin state of heme protein films, we discuss the EL spectra. As shown in Fig. 4, the EL spectra of myoglobin and cytochrome *c* are very much similar to each other. Then, we conclude that the broad feature of the EL spectra is attributable to the $S = 1/2$ low-spin state of heme. The EL spectrum of hemin in the LV state is completely different from that of myoglobin or cytochrome *c*. Since the hemin in the film is in the oxidized high-spin state as shown above, we conclude that the EL spectrum of hemin in the LV state is that of the oxidized high-spin state ($S = 5/2$). We can not directly determine the oxidation or spin state of hemin in the HV state. However, the comparison of an EL spectrum in the low-spin heme compounds (cytochrome *c* and myoglobin) with that in the high-spin compound (hemin in the LV state) suggests that the shape of an EL spectrum is another spin marker for heme compounds. Since the EL spectra of hemin in the HV state are very similar to those of the low-spin heme proteins, it seems reasonable to assume that hemin in the HV state is in the low-spin state. Very recently, we measured a soft X-ray absorption spectra of hemin in a BIODÉ, and found a change in the Fe 2p \rightarrow 3d transition by applying a voltage of 6 V to electrodes.¹⁷ Although detailed interpretation of the X-ray spectra has still not been completed, this result is consistent with the Fe spin-state change discussed above. Thus, the voltage-induced high-spin to low-spin transition is likely in hemin. Since hemin is a five-coordinated compound, addition of some axial ligands to iron is possible. If such addition occurs, the strength of the ligand-field changes, resulting in the high-spin to low-spin transition. According to magnetic susceptibility experiments by Bartoszek et al.,⁸ the effective magnetic moment is decreased when hemin powder is oriented in duacryl plus (cement). This suggests that the spin state of hemin is affected by chemical environments.

Finally, we will discuss the effect of impurities. In our experiments, we have studied EL in biomolecular compounds that do not exhibit PL. One may consider that fluorescent impurities contained in samples exhibit EL. For example, the porphyrin compounds containing Zn exhibit fluorescence.¹⁸ However, we performed PL experiments for all the biomolecular samples studied, and verified that PL in these compounds is too small to be detected. This indicates that impurities do not exhibit PL, even if they are contained.

Conclusion

We obtained the EL spectrum of a heme compound in the high-spin state for the first time. We revealed that the broad EL spectra obtained for myoglobin and cytochrome *c* is attributable to the heme in the low-spin state. We observed a voltage-induced transition in the ITO/hemin/Al junction. The transition is likely associated with the transition from the high-spin state to the low-spin state of iron in heme.

This work was supported by a Grant-in-Aid for Scientific Research on Priority Areas of Molecular Conductors (No. 15073207) from the Ministry of Education, Culture, Sports, Science and Technology, Japan.

References

- 1 P. S. Vincett, W. A. Barlow, R. A. Hann, G. G. Roberts, *Thin Solid Films* **1982**, 94, 171.
- 2 H. Tajima, S. Ikeda, M. Matsuda, N. Hanasaki, J. Oh, H. Akiyama, *Solid State Commun.* **2003**, 126, 579.
- 3 H. Tajima, S. Ikeda, K. Shimatani, M. Matsuda, Y. Ando, J. Oh, H. Akiyama, *Synth. Met.* **2005**, 153, 29.
- 4 K. Shimatani, H. Tajima, T. Komino, S. Ikeda, M. Matsuda, Y. Ando, H. Akiyama, *Chem. Lett.* **2005**, 34, 948.
- 5 S. Ikeda, H. Tajima, M. Matsuda, Y. Ando, H. Akiyama, *Bull. Chem. Soc. Jpn.* **2005**, 78, 1608.
- 6 I. Salmeen, G. Palmer, *J. Chem. Phys.* **1968**, 48, 2049.
- 7 a) A. Tasaki, J. Otsuka, M. Kotani, *Biochim. Biophys. Acta* **1967**, 140, 284. b) H. Hori, *Biochim. Biophys. Acta* **1971**, 251, 227. c) A. Ehrenberg, M. D. Kamen, *Biochim. Biophys. Acta* **1965**, 102, 333. d) D. M. Kurtz, *Comprehensive Coordination Chemistry II*, ed. by L. Que, W. B. Tolman, Elsevier, Amsterdam, **2003**, Vol. 8, pp. 229–260.
- 8 M. Bartoszek, M. Balanda, D. Skrzypek, Z. Drzazga, *Physica B* **2001**, 307, 217.
- 9 F. A. Walker, *Coord. Chem. Rev.* **1999**, 185–186, 471.
- 10 V. R. Marathe, S. Mitra, *J. Chem. Phys.* **1983**, 78, 915.
- 11 We also analyzed the magnetic susceptibility without using the data below 20 K. However, the obtained Curie constant, $C = 4.14 \text{ emu K mol}^{-1}$, was almost the same as that shown in the Table 1.
- 12 A similar analysis applied to cytochrome *c* gives us 95% of low-spin Fe^{III} ($S = 1/2$), and 5% of high-spin Fe^{III} ($S = 5/2$).
- 13 M. Feng, H. Tachikawa, *J. Am. Chem. Soc.* **2001**, 123, 3013.
- 14 C. W. Ong, Z. X. Shen, K. K. H. Ang, U. A. K. Kara, S. H. Tang, *Appl. Spectrosc.* **1999**, 53, 1097.
- 15 P. M. Callahan, G. T. Babcock, *Biochemistry* **1981**, 20, 952.
- 16 T. Kitagawa, Y. Kyogoku, T. Iizuka, M. I. Saito, *J. Am. Chem. Soc.* **1976**, 98, 5169.
- 17 I. Nakai, H. Kondo, T. Ohta, A. Doi, H. Tajima, unpublished.
- 18 H. Murakami, T. Kushida, *J. Lumin.* **1994**, 58, 172.